Changes in flow and wall stresses through arterial constrictions offset from the centre of the vessel

C. S. Chua[1] G. J. Sheard[2] K. Ryan[3] A. Fouras[4]

(Received 15 August 2008; revised 20 January 2009)

Abstract

Blood flow through small, obstructed vessels is studied by computing flows in tubes featuring three dimensional sinusoidal constrictions. A high order spectral element algorithm determines the extent of physiological flow characteristics such as recirculation zones and wall shear stress (WSS). Comparisons find that an increase in constriction eccentricity gives rise to more intense WSS. Moreover, these irregular flow conditions persist further downstream. Consistently, shear rate increases with Reynolds number and constriction eccentricity. Vorticity perpendicular to the constriction geometry and shear rate both increase with blockage ratio. In axisymmetric geometries, dissipation of the shear layers associated with downstream recirculation occurs more quickly. With larger constriction eccentricities, zones of high WSS are found on the far wall downstream of the constriction. This could lead to degradation of the wall tissue.

http://anziamj.austms.org.au/ojs/index.php/ANZIAMJ/article/view/1459 gives this article, © Austral. Mathematical Soc. 2009. Published January 29, 2009. ISSN 1446-8735. (Print two pages per sheet of paper.)

Contents

1 Introduction

Arterial disease is the leading cause of death in the developed world [1], yet only crude severity grading systems for stenotic blockages based on geometric features exist in medicine today. Furthermore, limited research has been conducted into fully three dimensional vessel constriction geometries [4].

A common form of arterial disease is atherosclerosis—a progressive, degenerative disease where plaques form on the arterial walls, comprising of an abnormal accumulation of inflammatory cells, lipids and connective tissues. Moreover, further complications occur, such as calcification of advanced lesions [12], or localised anaemia caused by constricted blood flow (ischaemia), leading to tissue infarction and ultimately death [13]. Thus the study of arterial fluid mechanics contributes significantly to medical research. The presence of an arterial constriction sees normal blood flow disturbed as the haemodynamics of the flow is influenced. The downstream flow will subse-

quently be more turbulent causing regions of high and low WSS to develop. Damage to the tissue may occur: high WSS and turbulence harms endothelial cells, activating platelets and causes plaque rupture [9]; whereas low WSS is associated with atherosclerotic plaque formation [3].

Currently there is no standardised procedure to accurately grade the physical severity of stenoses. Doctors often judge severity based on patient physical symptoms [11], as well as growth rate, constriction size, and supplementarily pressure drop [15]—often at high risk to patient lives.

Research into stenoses haemodynamics has accelerated in the field of engineering due to the increasing use of computational fluid dynamics (CFD), saving time and money whilst posing no threat to patients. However, much of the focus has been on two and three dimensional axisymmetric stenosis geometries or constricted flows between flat plates. Studies investigating flows through *non-axisymmetric* arterial constrictions have been rare.

Griffith et al. [5] conducted a two dimensional direct numerical simulation (DNS) study based on the hypothesis that flow over a semi-circular blockage between flat plates is analogous to flow over a backward facing step. They found recirculation regions that matched the vast array of experimental work. Recirculation regions cause flow stagnation which is detrimental to arterial health as it leads to a failure of dead cells to be transported. Clots form and induce infarction by occluding smaller arteries downstream [13].

Blackburn & Sherwin [1] investigated three dimensional pulsatile flow through axisymmetric stenoses. Vortex rings were found to shed from the stenosis across their flow velocity range, indicative of high WSS. From DNS studies performed by Jung et al. [6], pulsatile flows through three dimensional axisymmetric stenoses showed high WSS near the stenosed point due to the increased fluid velocity, indicative of plaque rupture [9].

It is unclear from these studies how asymmetric blockages effect flow, motivated by the observation that stenoses are rarely axisymmetric in practice. This investigation uses CFD to analyse flow characteristics by modelling dis-

eased arteries as pipes containing constrictions, focusing on changes to flow conditions as the severity and alignment of the constriction is varied.

2 Problem definition

Although blood displays non-Newtonian characteristics owing to the suspension of blood cells, it is commonplace to assume a Newtonian rheology when the vessel diameter is significantly larger than the cells within it [2]. As this study is concerned with stenoses that significantly impair the patient's health, our focus is on constrictions located on main blood vessels in the body, many orders of magnitude larger than blood cells. Branching and other curvature aspects of real blood vessels are also neglected to isolate the flow disturbance due to the stenosis. A uniform Poiseuille flow profile is input upstream, and the vessel is assumed rigid and impermeable, consistent with previous studies such as Liu et al. [10] and Blackburn & Sherwin [2].

The boundary conditions imposed on the model are

1. Constant reference pressure at the outlet,
2. Parabolic Poiseuille flow profile at the inlet,
3. Wall is rigid, impermeable,
4. Zero velocity at the walls,
5. Standard zero normal velocity gradient at the outlet.

Given vessel diameter D, and stenosis length L, this study uses an arbitrary stenosis length scale of $\mathsf{L}/\mathsf{D} = 2$, as depicted in Figures 1 and 2. The stenosis is located $5\mathsf{D}$ downstream of the inlet, giving enough upstream length to avoid disturbing the flow through the constriction. The domain extends $10\mathsf{D}$ downstream to permit recirculation zones to be resolved.

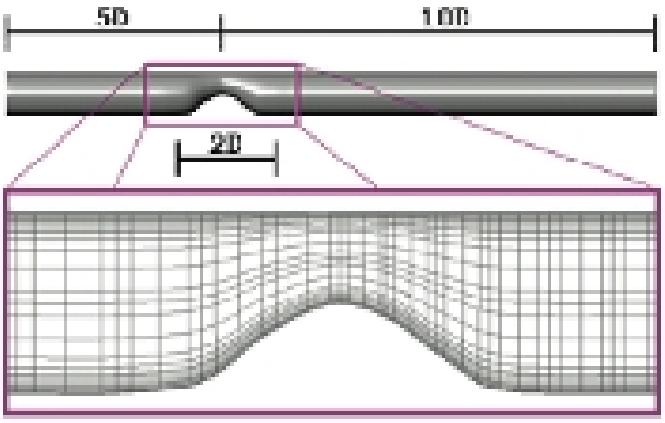

FIGURE 1: The full computational domain showing the nodal mesh elements at the stenosed region for the most eccentrically positioned geometry.

Meshes for all geometries consist of 784 elements, with higher element density in the vicinity of the obstruction as well as near the walls.

The blockage ratio is expressed as the reduction from the artery diameter to the minimum stenotic diameter, $1 - d/D$. The blockage ratios investigated ranged from 0 (no stenosis) to 0.5. The stenosis eccentricity is the offset of the constriction towards one side of the pipe. It is defined in this study as the fractional shift of the stenosis centreline from the vessel centreline in the positive y-direction, and given as a ratio of D (E/D). An axisymmetric stenosis has no deviation and yields zero eccentricity, as shown in Figure 2 (left). A stenosis with $d/D = 0.5$ can have an eccentricity up to half that value, at $E/D = 0.25$, as shown in Figure 2 (right).

The flow is considered to be governed by the incompressible Newtonian Navier–Stokes equations: $\rho\vec{g} - \nabla p + \nabla \cdot \tau_{ij} = \rho D\vec{u}/Dt$, where $\vec{g}$ is gravity, p is the scalar pressure field, ∇ is the gradient operator, τ_{ij} is the viscous stress tensor, $\vec{u}$ is the velocity vector, and t is time. The fluid also satisfies conversation of mass: $\partial\rho/\partial t + \nabla \cdot (\rho\vec{u}) = 0$. The Reynolds number is

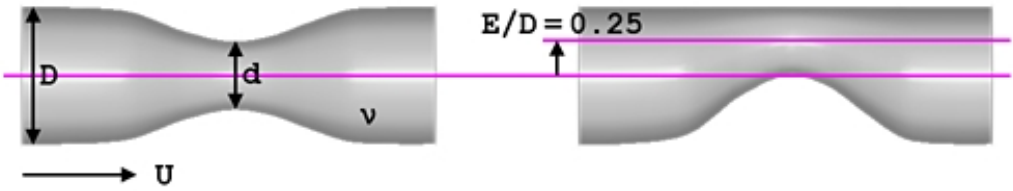

FIGURE 2: Model parameters showing $E/D = 0$ (left), and $E/D = 0.25$ (right).

$Re = UD/\nu$, where D is the pipe diameter, U is the fluid velocity, and ν is the kinematic viscosity of blood. A Reynolds number range up to $Re = 500$ is investigated in this study. One of the flow parameters of particular interest in this study is vorticity, the curl of the fluid velocity: $\vec{\omega} = \nabla \times \vec{v}$.

3 Numerical method

This CFD study is conducted using an in-house, incompressible and unsteady Navier–Stokes solver, which was employed and validated by Sheard and Ryan [14]. The code utilises a spectral element method for spatial discretization, using high order polynomial functions to approximate the flow solution within each element [8]. Varying the spectral element polynomial order allows spatial refinement of the model without modifying the mesh. A polynomial order of five is used for this study, set by computational RAM limitations. A grid independent study found a polynomial order of five to yield an accuracy to within 0.003% of the calculated grid independent value. A third order, backwards multistep, scheme is employed for the temporal discretization, which is particularly favourable for solving stiff problems [7].

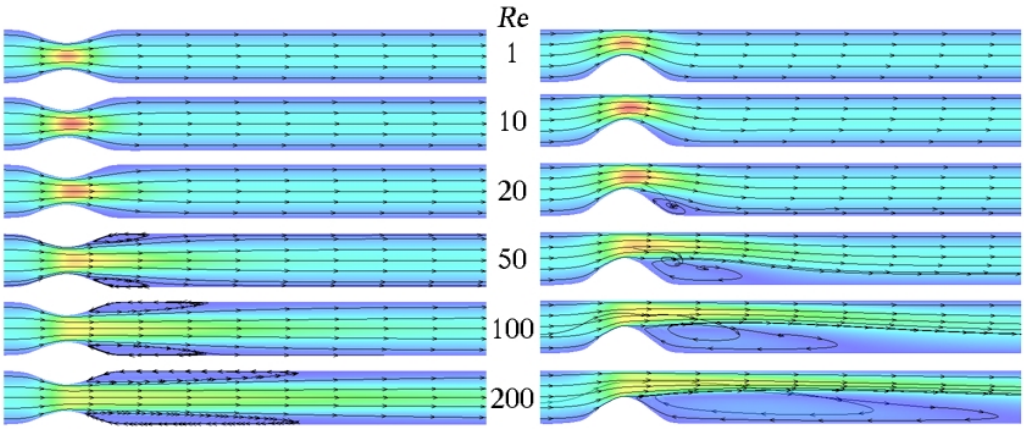

FIGURE 3: Velocity magnitude and streamtraces at $z = 0$ slices, through increasing upstream Re at $d/D = 0.5$, for $E/D = 0$ (left) and $E/D = 0.25$ (right). The flow domain shown extends from $1.5D$ upstream of the stenosis throat, to $8.0D$ downstream.

4 Results

An L_2 norm defined $L_2 = \int_\Omega |U|\, d\Omega$, where U is the velocity vector field, and Ω is the computational domain, is monitored for spatial convergence. The L_2 norm calculated with polynomial order of five is within 0.003% of the extrapolated grid independent value, at $Re = 100$ and $d/D = 0.5$. Tests indicate that a high degree of accuracy is preserved up to $Re = 500$, therefore $n = 5$ is implemented in this study.

4.1 Varying Reynolds number

The effect of varying Re is investigated for two models with $d/D = 0.5$; one with $E/D = 0$, the other with $E/D = 0.25$. Figure 3 shows that the onset of

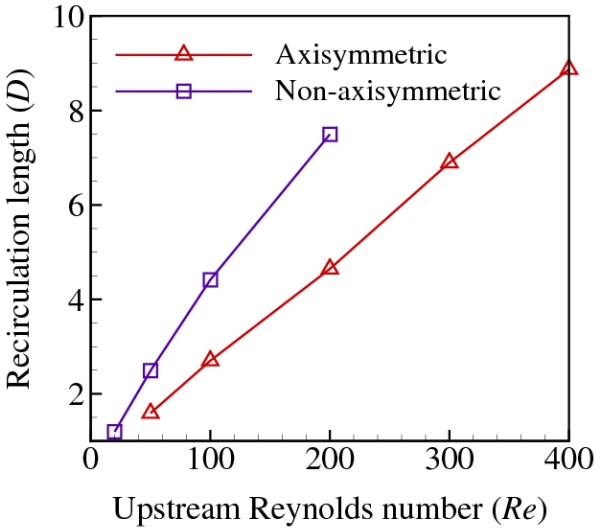

FIGURE 4: Recirculation length plotted against upstream Re at d/D = 0.5, for both E/D = 0 (axisymmetric) and E/D = 0.25 (non-axisymmetric). The data is truncated at Re = 400 (axisymmetric) and Re = 200 (non-axisymmetric) since recirculation regions beyond these Reynolds numbers extend past the computational domain of 10D downstream.

the recirculation region appears earlier for the non-axisymmetric geometry. This is expected since the eccentricity denotes more curvature of the pipe to one side which induces higher shear as the flow accelerates through the constriction. The length and width of the recirculation is also longer and wider for the corresponding Re.

Figure 4 indicates that the recirculation region is significantly longer for the non-axisymmetric stenosis, and has a faster growth rate as seen by the steeper gradient. Recirculation length appears to scale with Re and local constriction height.

4.2 Varying eccentricity

Models with $d/D = 0.5$ and $0 \leq E/D \leq 0.25$ are computed at Reynolds numbers of 100 and 500, through 0.05 increments. The general trends of the $Re = 500$ models followed suit to the $Re = 100$ models, and the average difference in values matches up with the results attained from the Reynolds number study; vorticity in all components and shear rate are higher, with increasing Re. Again, this finding suggests that non-axisymmetric stenoses should be treated with more care and diligence than axisymmetric stenoses, as the associated flow conditions experienced by the patient are more severe.

The shear rate magnitude is computed using the leading eigenvalue of the shear rate tensor $\partial v_i/\partial x_j + \partial v_j/\partial x_i$, with velocity gradients expressed in tensor notation. Figure 5 shows the shear rate magnitude: high shear regions are located at the stenosis throat. With increasing eccentricity, these high shear regions, which initially dissipate in the lumen, migrate to the wall opposite the throat, signifying potential damage to the arterial wall.

Figure 6 (left) shows that with increasing eccentricity, the shear rate magnitude increases at the throat but decreases at the wall directly opposite, as the high speed jet of fluid moves downstream. This corresponds to the linearly increasing shear rate magnitude measured at the opposite wall 1D down-

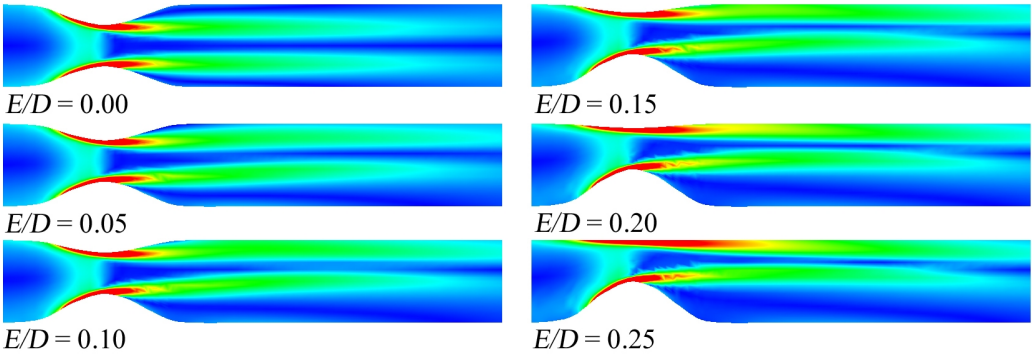

FIGURE 5: Shear rate magnitude contours in $z = 0$ slices at varying eccentricities. $d/D = 0.5$ and $Re = 500$. The flow domain shown extends from $1.25D$ upstream of the stenosis throat, to $4.75D$ downstream.

stream, as seen in Figure 6 (right).

4.3 Varying blockage ratio

The effect of varying blockage ratio is investigated for axisymmetric and non-axisymmetric models at $Re = 500$, with eccentricity ratio ranging between $0 \leq E/D \leq 0.25$. From the results, vorticity in the model's reflective symmetry plane (z-component of vorticity) is the most prominent flow parameter exhibited. x-components (streamwise) and y-components of vorticity are negligible across the analysed blockage ratios. Figure 7 (left) shows an increase in the z-component of vorticity at the throat with increasing blockage ratio for both axisymmetric and non-axisymmetric models, consistent with Jung et al. [6] who found there was an exponential increase in velocity with increasing blockage ratio. Figure 7 (right) shows that the axisymmetric model dissipates z-component of vorticity $1D$ downstream of the constriction, but the non-axisymmetric model follows the trend at the throat; increasing z-component of vorticity with increasing blockage ratio, signifying it persists

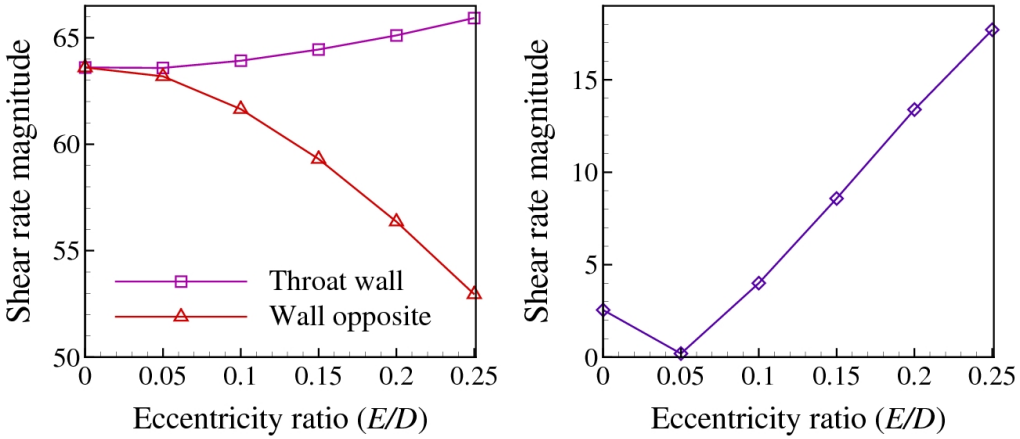

FIGURE 6: Shear rate magnitude plotted against E/D (d/D = 0.5 and Re = 100), at both sides of the throat (left), and wall opposite the throat 1D downstream of the stenosis (right). Shear rate magnitude was normalised by U/D.

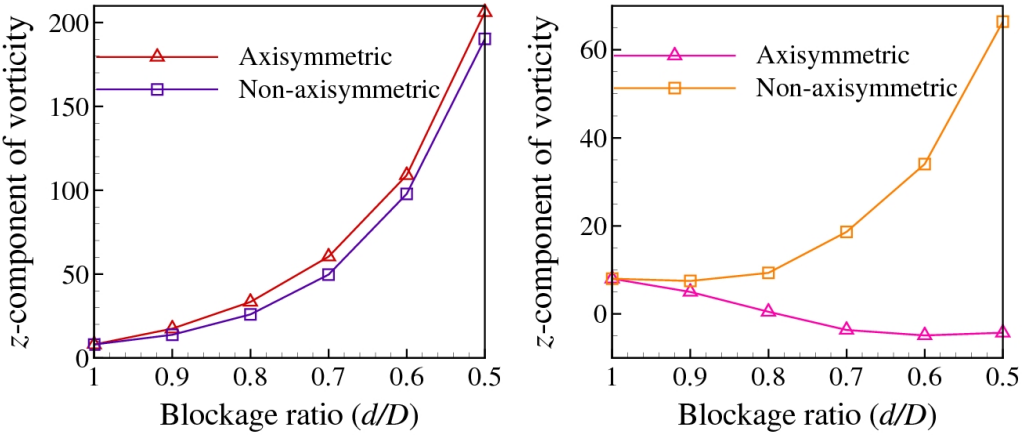

FIGURE 7: z-component of vorticity plotted against d/D at $Re = 500$, for both $E/D = 0$ (axisymmetric) and $E/D = 0.25$ (non-axisymmetric) on the opposite wall, at the throat (left), and $1D$ downstream of the throat (right).

at the downstream wall.

Figure 8 plots slices at several locations through the models. They further illustrate the vastly different flow structure downstream of the stenoses between the axisymmetric and non-axisymmetric models. The vorticity in the axisymmetric case is completely symmetrical as the flow moved downstream, dissipating within the lumen of the artery. This demonstrates that a high speed jet of fluid extends downstream along the vessel centreline. As for the non-axisymmetric case, the eccentrically positioned stenosis pushes the vorticity against the opposite wall as it travels downstream, causing high z-component vorticity at the downstream wall.

Once again, the non-axisymmetric model experiences adverse flow conditions to a higher degree than the axisymmetric case, reaffirming the notion that physiological predictions surrounding non-axisymmetric arterial constrictions should not be based on axisymmetric observations or data.

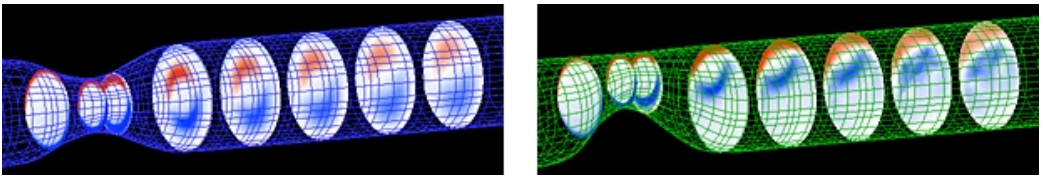

FIGURE 8: z-component of vorticity contours on x-plane slices at $d/D = 0.5$ and $Re = 500$, for $E/D = 0$ (left) and $E/D = 0.25$ (right). Flow is left to right.

5 Conclusions

This article presents the first systematic study of fluid flow through fully three dimensional, offset stenoses in cylindrical tubes. The findings conclude that flow conditions experienced by non-axisymmetric models are more intense than axisymmetric models. The eccentrically positioned stenoses give rise to larger stagnation regions as well as more intense flow characteristics, generally exhibiting higher and lower WSS and vorticity in the reflective symmetry plane, at the wall immediately downstream of the stenosis. Furthermore, these flow patterns persist further downstream. Conclusions drawn from axisymmetric investigations into arterial disease should not be used to judge the physiological severity of non-axisymmetric stenoses.

The parameter scope investigated in this study is bounded by computational limitations, but serves as a solid basis for continuing research into non-axisymmetric stenoses. In particular, it is difficult to make predictions about an inherently transient problem with a steady state model. The effect of pulsatile in-flow is currently under investigation.

Acknowledgements This research was supported under the Monash Research for an Ageing Society Support Scheme. The Australian Partnership for Advanced Computing was utilised for this study, thanks to a Merit Allocation Scheme time allocation.

References

[1] Blackburn, H. M. & Sherwin, S. J., Three-dimensional instabilities and transition of steady and pulsatile axisymmetric stenotic flows, *J. Fluid Mech.*, **533**, 2005, 297–327. doi:10.1017/S0022112005004271 C745, C746

[2] Blackburn, H. M & Sherwin, S. J., Instability modes and transition of pulsatile stenotic flow: pulse-period dependence, *J. Fluid Mech.*, **573**, 2007, 57–88. doi:10.1017/S0022112006003740 C747

[3] Chytilova, E., Malik, J., Kasalova, Z., Dolezalova, R., Stulc, T., & Ceska, R., Lower wall shear rate of the common carotid artery in treated type 2 diabetes mellitus with metabolic syndrome, Accepted for publication in *Physiological Research*, 2008. http://www.biomed.cas.cz/physiolres/pdf/prepress/1445.pdf C746

[4] Dodds, S. R, The Haemodynamics of Asymmetric Stenoses, *Eur. J. Vasc. Endovasc. Surg.*, **24**, 2002, 332–337. doi:10.1053/ejvs.2002.1729 C745

[5] Griffith, M. D., Hourigan, K. & Thompson, M. C., Numerically Modelling Blockage Effects on the Flow between Flat Plates, *15th Australasian Fluid Mechanics Conference*, 2004, The University of Sydney, Sydney, Australia. http://www.aeromech.usyd.edu.au/15afmc/proceedings/papers/AFMC00103.pdf C746

[6] Jung, H., Choi, J. W., & Park, C. G., Asymmetric Flows of non-Newtonian Fluids in Symmetric Stenosed Artery, *Korea-Australia Rheology J.*, **16**, 2004, 101–108. http://www.rheology.or.kr/down/16-2(6).pdf C746, C753

[7] Karniadakis, G. E., Orszag, S. A. & Israeli, M., High-order splitting methods for the incompressible Navier–Stokes equations, *J. Comput.*

Phys., **97**, 1991, 414–443. doi:10.1016/0021-9991(91)90007-8 C749

[8] Karniadakis, G. E. & Sherwin, S. J., 2005, *Spectral/hp Element Methods for CFD*, 2nd ed., Oxford University Press, Oxford. C749

[9] Li, M. X., Beech-Brandt, J. J., John, L. R., Hopkins, P. R., & Easson, W. J., Numerical analysis of pulsatile blood flow and vessel wall mechanics in different degrees of stenoses, *Journal of Biomechanics*, **40**, 2007, 3715–3724. doi:10.1016/j.jbiomech.2007.06.023 C746

[10] Liu, G. T., Wang, X. J., Ai, B. Q. & Liu, L. G., Numerical study of pulsating flow through a tapered artery with stenosis, *Chinese Journal of Physics*, **42**, 2004, 401–409. http://psroc.phys.ntu.edu.tw/cjp/v42/401.pdf C747

[11] NHS Direct, 2006, *Coronary Angioplasty*, BMJ Publishing Group Ltd, England & Wales, National Health Service clinical evidence for patients. http://besttreatments.bmj.com/btuk/pdf/18627.pdf C746

[12] Ridker, P. M., On evolutionary biology, inflammation, infection, and the causes of atherosclerosis, *Circulation*, **105**, 2002, 2–4. http://circ.ahajournals.org/cgi/reprint/105/1/2 C745

[13] Ross, R., Cell Biology of Atherosclerosis, *Annu. Rev. Physiol.*, **57**, 1995, 791–804. doi:10.1146/annurev.ph.57.030195.004043 C745, C746

[14] Sheard, G. J. & Ryan, K., Pressure-driven flow past spheres moving in a circular tube, *J. Fluid Mech.*, **592**, 2007, 233–262. doi:10.1017/S0022112007008543 C749

[15] Thomas, S. M., The current role of catheter angiography, *Imaging*, **13**, 2001, 366–375. http://imaging.birjournals.org/cgi/content/full/13/5/366 C746

Author addresses

1. **C. S. Chua**, Div. Biological Engineering, Monash University, Victoria 3800, Australia; and Fluids Laboratory for Aeronautical & Industrial Research, Dept. Mechanical and Aerospace Engineering, Monash University, Victoria 3800, Australia.
mailto:Charlene.Chua@eng.monash.edu.au

2. **G. J. Sheard**, Div. Biological Engineering, Monash University, Victoria 3800, Australia; and Fluids Laboratory for Aeronautical & Industrial Research, Dept. Mechanical and Aerospace Engineering, Monash University, Victoria 3800, Australia.

3. **K. Ryan**, Fluids Laboratory for Aeronautical & Industrial Research, Dept. Mechanical and Aerospace Engineering, Monash University, Victoria 3800, Australia.

4. **A. Fouras**, Div. Biological Engineering, Monash University, Victoria 3800, Australia; and Fluids Laboratory for Aeronautical & Industrial Research, Dept. Mechanical and Aerospace Engineering, Monash University, Victoria 3800, Australia.